PERGAMON

International Journal of Solids and Structures 40 (2003) 4501–4517

INTERNATIONAL JOURNAL OF SOLIDS and STRUCTURES

www.elsevier.com/locate/ijsolstr

Stability of sandwich plates by mixed, higher-order analytical formulation

J.B. Dafedar [a], Y.M. Desai [a,*], A.A. Mufti [b]

[a] *Department of Civil Engineering, Indian Institute of Technology Bombay, Powai, Mumbai 400 076, India*
[b] *Department of Civil Engineering, The University of Manitoba, Winnipeg, Man., Canada R3T 5V6*

Received 26 July 2002; received in revised form 12 April 2003

Abstract

A unified mixed, higher-order analytical formulation has been presented in this paper to predict general buckling as well as wrinkling of a general multi-layer, multi-core sandwich plate having any arbitrary sequence of stiff layers and cores. Assumptions of thin stiff layers and anti-plane core, which are usually made in the analysis of sandwiches, have been eliminated in the present formulation. Displacements as well as the transverse stress continuities have been enforced in the formulation by incorporating them as the degrees-of-freedom. The modal transverse stresses have been obtained directly as eigen vectors and thus their separate calculations have been advantageously avoided. Two sets of mixed models have been proposed on the basis of individual layer as well as equivalent single layer (ESL) theories by selectively incorporating non-linear components of Green's strain tensor. Solutions from the models have been shown to be in excellent agreement with the available three-dimensional elasticity solutions as well as with the available experimental results. It has been demonstrated that the ESL theories cannot accurately evaluate the overall buckling as well as the wrinkling loads of sandwiches. Limitations of the typical simplifying assumptions have also been highlighted.

Keywords: Buckling; Higher-order theory; Local buckling; Mixed theory; Sandwich plates; Stability; Wrinkling

1. Introduction

Sandwich plates have been used widely in aerospace, shipbuilding, construction and other industries because of their lightweight, high stiffness, durability and high structural efficiency. The use of fiber reinforced composite face sheets reduces thermal conductivity through thickness, therefore such sandwiches can withstand high service temperature.

Sandwich panels subjected to in-plane compressive forces may buckle in various modes depending on the material properties of the face sheets as well as the core and their relative stiffnesses. Sandwiches may exhibit: (i) global or general buckling, (ii) face-sheet wrinkling, (iii) face-sheet dimpling (for discontinuous

* Corresponding author. Tel.: +91-22-576-7333/7301; fax: +91-22-576-7302.
E-mail address: desai@civil.iitb.ac.in (Y.M. Desai).

0020-7683/03/$ - see front matter © 2003 Published by Elsevier Ltd.
doi:10.1016/S0020-7683(03)00283-X

or honeycomb core); and (iv) shear crimpling. Further, delamination of faces may also occur from the core if the bond strength is poor.

A review of literature on the modeling, analysis and design of sandwich plates has been presented by Noor and Burton (1996). The three-dimensional elasticity solutions for general buckling of simply supported sandwich panels with composite face sheets have been presented by Noor et al. (1994). The sandwich panels were analyzed for combined temperature change and the uniform edge compression.

Analytical approaches available in the literature are usually based on the following typical simplifying assumptions:

(i) The transverse normal stress (σ_z) is very small in the face sheets as well as in the core.
(ii) Faces are thin panels that are perfectly rigid for the out-of-plane shear. Therefore, the faces have only the flexural strength and the in-plane shear rigidity.
(iii) The core is typically anti-plane, i.e. it only has finite out-of-plane shear rigidities.

A comprehensive work on sandwich construction has been presented by Allen (1969), wherein the zigzag deformation pattern or a three-layered model was used for the analysis of sandwich beams and plates. However, the analysis was based on the first-order shear deformation theory. The early works of Benson and Mayers (1967) and Pearce and Webber (1971) dealt with the symmetric and anti-symmetric modes of buckling, which were analyzed separately. Benson and Mayers (1967) investigated the general stability and face wrinkling modes of sandwich panels by applying the variational principle to potential energy of a panel. The Lagrange multipliers were used to introduce face core continuity. Pearce and Webber (1971) obtained the overall buckling and wrinkling loads for sandwich plates with orthotropic faces and core. Hunt et al. (1988) and Hunt and Da Silva (1990) used an approach based on energy methods and superposition of symmetric and asymmetric modes. However, the approach was restricted to certain configurations and boundary conditions. Sandwich plate buckling problems have also been evaluated analytically by Rao (1985), Kim and Hong (1988), Ko and Jackson (1993), Aiello and Ombres (1997) and Hadi and Matthews (1998, 2000).

Higher-order shear deformation theories are being applied to sandwich construction recently. Frostig (1998), for example, obtained general as well as local buckling loads for sandwich panels consisting of two faces and a soft orthotropic core. However, the analysis was based on the above-mentioned simplifying assumptions. Kant and Swaminathan (2000) have also presented a displacement based higher-order formulation in which the above mentioned simplifying assumptions were eliminated. However, the formulation was based on an equivalent single layer (ESL) theory, which cannot accurately predict the local buckling modes.

Majority of these efforts have been confined to single core construction with two facings. The stability problem of multi-core sandwich plates has been comparatively less explored despite their wide application in the aircraft industry. Wong and Salama (1967) obtained series solutions by using the Lagrange formulation of variational calculus in which a common shear angle was assumed for all the core layers. Chan and Foo (1977) presented a finite strip method (FSM) for multi-layer sandwich plates.

An extensive literature survey reveals that the buckling analysis of sandwich plates is invariably based on some simplifying assumptions in either material behavior and/or in modeling their structural behavior. Moreover, higher-order theories have been applied to analyze the sandwich plates having single core. Majority of the approaches consider the general and local buckling modes to be uncoupled. The objective of the present paper is to fill these gaps in the literature and to present a unified approach based on the mixed higher-order theory that can predict both general as well as wrinkling modes of buckling. Further, the above-mentioned simplifying assumptions have been advantageously eliminated for general multi-layer sandwiches having any number of cores and stiff layers placed arbitrarily. The theory is applicable especially to orthotropic sandwich plates.

Recently, the authors (Dafedar and Desai, 2002) have presented a mixed higher-order formulation by considering six degrees-of-freedom (DOF), viz. three displacement components, u, v and w (along x, y and z directions, respectively) and three transverse stress components, τ_{xz}, τ_{yz} and σ_z. These transverse stresses have been invoked from the assumed displacement fields by using the constitutive law. Equilibrium equations have been derived by using the minimum potential energy principle. Thus, the method presented differs from the other higher-order theories in following ways. It is based on the minimum potential energy principle. The method explicitly satisfies the requirements of through-thickness continuity of transverse stress components and continuous displacement fields as both are incorporated in the DOF. Further, the fundamental elasticity relations between stress and displacement fields have been maintained at all points of an elastic continuum. Moreover, it enables the direct computation of the transverse stress components as eigenvectors.

Two sets of mixed models HYF1 and HYF2 have been presented by selectively incorporating non-linear components of Green's strain tensor. Individual layer theory (ILT) based HYF1 models have been formulated by considering a local cartesian co-ordinate system at the mid-surface of each individual layer. Six DOF are assigned to bottom as well as top surfaces of each individual layer. The condition of traction-free surface has not been enforced in the models for a consistent comparison with the data available in the literature. Therefore, the total number of DOF in HYF1 always equals $[(N+1)\times 6]$ for N layered sandwich plate. Finer discretization of layers in z-direction in HYF1 models leads to transverse stresses that are close to zero indicating traction free surfaces. On the other hand, the global mixed models HYF2 have been formulated by considering cartesian co-ordinate system at the mid-surface of entire sandwich and by assigning six DOF to bottom as well as top surface of the entire plate. Hence, total number of DOF always remains 12 in HYF2 models. The two mixed models have been applied in this paper to a general multilayer, multi-core sandwich plate having any arbitrary sequence of stiff layers and cores.

2. Formulation

A rectangular sandwich plate of plan dimensions L_x by L_y and thickness H has been considered as shown in Fig. 1. The sandwich is composed of uniform thickness layers of homogeneous and orthotropic material. Any number of stiff layers and core are assumed to be placed arbitrarily. Three-displacement components $u(x,y,z)$, $v(x,y,z)$ and $w(x,y,z)$ at any point in a lamina can be expanded in terms of thickness coordinate, z, by using the Taylor's series expansion as

$$u_k(x,y,z) = \sum_{j=0}^{3} z^j a_{kj}(x,y) \tag{1}$$

Here, u_k $(k=1,2,3)$ represent three displacement components, u, v, w, respectively and a_{kj} indicate the generalized co-ordinates.

2.1. Constitutive law

Each lamina in a sandwich has been considered to be in a three-dimensional state of stress. Constitutive relations for a typical ith orthotropic lamina can be expressed as

$$\{\sigma\}^i = [C]^i\{\varepsilon\}^i \tag{2}$$

Here, $\{\sigma\}^i$ and $\{\varepsilon\}^i$ are stresses and the linear strain components, respectively, referred to the lamina co-ordinates and $[C]^i$ represents a matrix of elastic constants of the ith lamina.

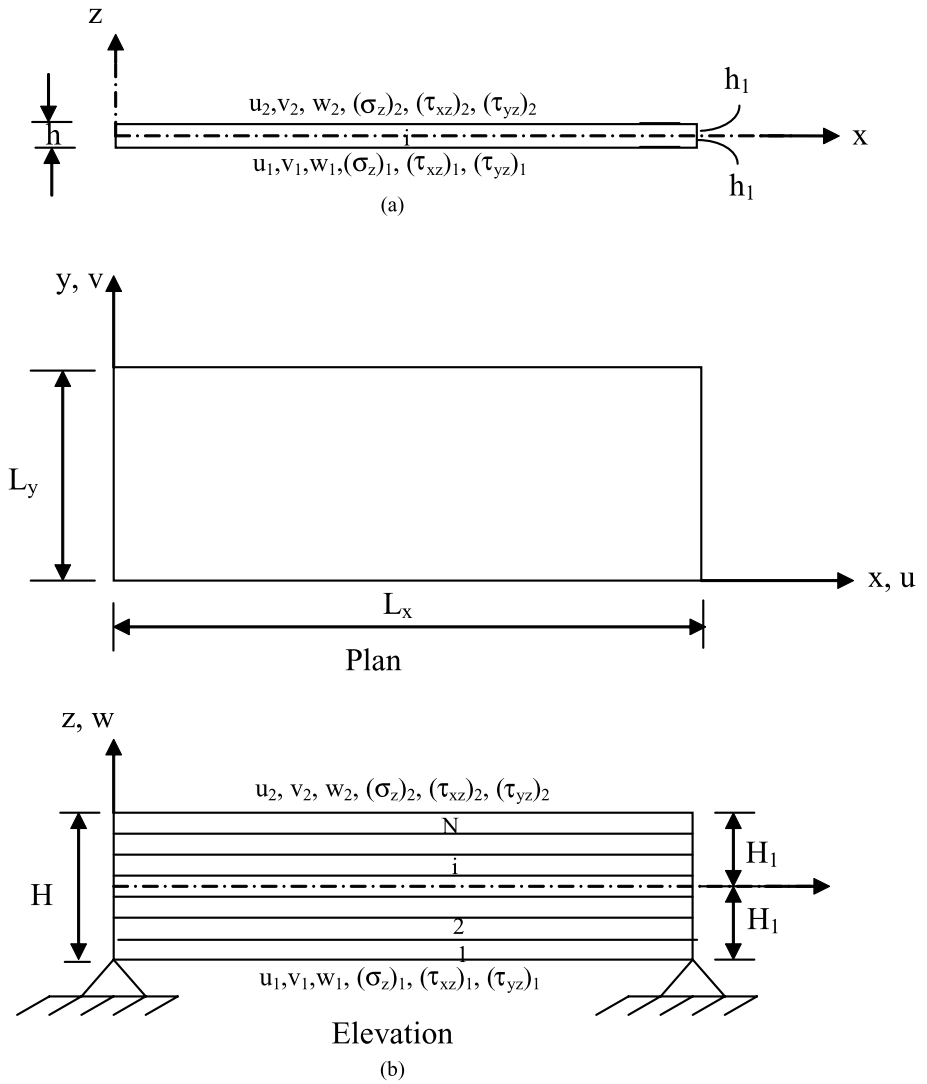

Fig. 1. Sandwich plate geometry, co-ordinate axes and DOF for: (a) *i*th layer of a sandwich plate in conjunction with HYF1 model; (b) sandwich plate.

2.2. Green's strain tensor

Following components of Green's strain tensor have been considered in the analysis.

$$\begin{aligned}
\varepsilon_x &= u' + \tfrac{1}{2}[\delta_1(u')^2 + \delta_2(v')^2 + \delta_3(w')^2] \\
\varepsilon_y &= v^* + \tfrac{1}{2}[\delta_1(u^*)^2 + \delta_2(v^*)^2 + \delta_3(w^*)^2] \\
\varepsilon_z &= \overline{w} \\
\gamma_{xy} &= u^* + v' + \delta_1(u'u^*) + \delta_2(v'v^*) + \delta_3(w'w^*) \\
\gamma_{yz} &= w^* + \overline{v} \\
\gamma_{xz} &= \overline{u} + w'
\end{aligned} \tag{3a}$$

$$\{\varepsilon\} = \{\varepsilon\}_{\mathrm{L}} + \{\varepsilon\}_{\mathrm{NL}} \tag{3b}$$

where $'$, * and bar atop a character indicate derivatives with respect to x, y and z directions, respectively. The linear part of strain–displacement relations $\{\varepsilon\}_{\mathrm{L}}$ has been used to derive the lamina property matrices. On the other hand, the non-linear strain–displacement relations $\{\varepsilon\}_{\mathrm{NL}}$ have been employed to derive the geometric property matrices of a lamina. Laminates do not buckle under the application of external stresses in z-direction (σ_z) and the transverse shear stresses τ_{xz} and τ_{yz}. Therefore, the non-linear terms from the strains ε_z, γ_{xz} and γ_{yz} will not contribute to the work done by external stresses. Hence, these non-linear terms are not included in Eq. (3a). Hybrid models HYF1j and HYF2j ($j = 0, 1, 2, 3$) have been defined based on values of the Kronecker deltas δ_1 to δ_3 used in Eqs. (3a) as follows.

(i) HYF13 and HYF23—$\delta_1 = \delta_2 = \delta_3 = 1$,
(ii) HYF12 and HYF22—$\delta_1 = \delta_3 = 1$; $\delta_2 = 0$,
(iii) HYF11 and HYF21—$\delta_1 = 0$, $\delta_2 = \delta_3 = 1$, and
(iv) HYF10 and HYF20—$\delta_1 = \delta_2 = 0$; $\delta_3 = 1$.

It can be noted from Eq. (3a) that the Von-Karman strain–displacement relations have been utilized in models HYF10 and HYF20. Further, contributions of non-linear strains terms related with the u and v displacements have been neglected in most theories available in the literature to simplify analysis.

2.3. Kinematics

Constitutive Eqs. (2) have been utilized in the description of kinematics to introduce the transverse stresses as DOF. The stress–displacement expressions have been derived by substituting Eq. (1) in the linear part of the strain–displacement relations shown in Eq. (3a). The ensuing equation is then substituted into the Eq. (2). Consequently, equations for the stress DOF have been derived by substituting, $z = \pm\zeta$ in the resulting equations. Here, ζ is half the thickness of ith lamina (h_1) for all individual layer mixed models (HYF1), or half the thickness of entire sandwich (H_1) for all HYF2 models. Similarly, the equations for displacement DOF can be derived by substituting $z = \pm\zeta$ in equation set (1). By solving two sets of equations simultaneously, the generalized co-ordinates are expressed in terms of the DOF. Thus, the displacement field can be expressed in terms of DOF as

$$\begin{Bmatrix} u \\ v \\ w \end{Bmatrix} = [N_1]\{q\} + [N_2]\{q\}' + [N_3]\{q\}^* \tag{4}$$

Here, $[N_1]$, $[N_2]$ and $[N_3]$ are 3×12 shape function matrices (Dafedar and Desai, 2002). On the other hand, $\{q\}$ is a vector of DOF given by

$$\{q\} = \{\, u_r \quad (\tau_{xz})_r \quad w_r \quad (\sigma_z)_r \quad v_r \quad (\tau_{yz})_r \quad u_s \quad (\tau_{xz})_s \quad w_s \quad (\sigma_z)_s \quad v_s \quad (\tau_{yz})_s \,\}^{\mathrm{t}} \tag{5}$$

Subscripts 'r' and 's' in Eq. (5) indicate bottom and top surface of ith layer in all HYF1 models. However, they represent the bottom and top surfaces of the entire sandwich in all HYF2 models.

2.4. Strain–displacement relations

Substitution of Eqs. (4) in linear part of Eqs. (3a) yields the linear strain–displacement equation

$$\{\varepsilon\}_{\mathrm{L}} = [a]\{q\} + [b]\{q\}' + [d]\{q\}'' + [e]\{q\}^* + [f]\{q\}^{**} + [g]\{q\}^{*\prime} \tag{6}$$

where $[a]$, $[b]$, $[d]$, $[e]$, $[f]$ and $[g]$ are 6×12 nodal strain–displacement matrices that can be derived from the shape function matrices.

By substituting Eqs. (4) into the non-linear parts of Eqs. (3a), the relevant non-linear strain terms can be expressed as

$$\begin{aligned}\left(\frac{\partial u_k}{\partial x}\right)^2 &= [\{N_1(k,j)\}\{q\}' + \{N_2(k,j)\}\{q\}'' + \{N_3(k,j)\}\{q\}^{*\prime}]^2\\ \left(\frac{\partial u_k}{\partial y}\right)^2 &= [\{N_1(k,j)\}\{q\}^{*} + \{N_2(k,j)\}\{q\}'^{*} + \{N_3(k,j)\}\{q\}^{**}]^2\end{aligned} \tag{7}$$

where $\{N_p(k,j)\}$ ($p=1,2,3$ and $j=1$–12) indicate kth row of the 3×12 shape function matrices. Eqs. (4), (6) and (7) are the general equations representing displacements, linear strains and the relevant non-linear strains respectively, at any point in the sandwich.

2.5. Potential energy of a lamina

The potential energy, Π^i, of a typical ith layer enclosing a space volume, V, can be expressed as

$$\Pi^i = U^i - W^i \tag{8}$$

where U^i represents the strain energy stored in the lamina and W^i indicates the work done by externally applied stresses σ_x^{pi} and σ_y^{pi} acting in the x and y directions, respectively. By substituting the expressions for strain energy and the work done in Eq. (8), the potential energy of a lamina can be written as

$$\Pi^i = \frac{1}{2}\int_v \{\varepsilon\}_L^T [C]^i \{\varepsilon\}_L \,dv - \left[\int_v \sigma_x^{pi}(\varepsilon_x)_{NL}\,dv + \int_v \sigma_y^{pi}(\varepsilon_y)_{NL}\,dv\right] \tag{9}$$

2.6. Lamina equations

Following trial solutions have been considered, which satisfy simple support conditions.

$$\begin{aligned} u_j &= A_j \cos\lambda_1 x \sin\lambda_2 y \quad (\tau_{xz})_j = B_j \cos\lambda_1 x \sin\lambda_2 y\\ w_j &= C_j \sin\lambda_1 x \sin\lambda_2 y \quad (\sigma_z)_j = D_j \sin\lambda_1 x \sin\lambda_2 y\\ v_j &= E_j \sin\lambda_1 x \cos\lambda_2 y \quad (\tau_{yz})_j = F_j \sin\lambda_1 x \cos\lambda_2 y, \qquad j = r,s \end{aligned} \tag{10}$$

Here, $\lambda_1 = m\pi/L_x$, $\lambda_2 = n\pi/L_y$, m and n are the wave numbers indicating a specific buckling mode.

By substituting equation set (10) into Eq. (9), the ensuing equation can be obtained by applying variational principle as

$$\left[[K]^i - \sigma_x^{pi}[K_{G1}]^i - \sigma_y^{pi}[K_{G2}]^i\right]\{q_a\} = 0 \tag{11}$$

where

$$\{q_a\} = \{A_r \quad B_r \quad C_r \quad D_r \quad E_r \quad F_r \quad A_s \quad B_s \quad C_s \quad D_s \quad E_s \quad F_s\}^t \tag{12}$$

2.7. Global equations

2.7.1. HYF1—individual layer models

Matrices $[K^i]$ and $[K_G]^i$ of various laminae are assembled by enforcing continuities of displacements and the transverse stresses at the interfaces of the laminae to form the global matrices $[K]$ and $[K_G]$ for the entire sandwich plate. The global equations can then be written as

$$[K] - \lambda_{cr}[K_G] = [0] \tag{13a}$$

where

$$[K_G] = \sigma_x^p[K_{G1}] + \sigma_y^p[K_{G2}] \tag{13b}$$

The critical buckling coefficient λ_{cr} can be evaluated by employing a generalized eigenvalue solver. Subsequently, the buckling stresses can be expressed as

$$\sigma_{xcr}^p = \lambda_{cr}\sigma_x^p \quad \text{and} \quad \sigma_{ycr}^p = \lambda_{cr}\sigma_y^p.$$

2.7.2. HYF2—equivalent single layer models

Global matrices of the entire sandwich are evaluated by summing the respective matrices of all the laminae for HYF2 models as

$$[K] = \sum_{i=1}^{N}[K]^i \quad \text{and} \quad [K_G] = \sum_{i=1}^{N}[K_G]^i \tag{14}$$

By substituting these global matrices in Eq. (13a), the critical buckling coefficient λ_{cr} can be evaluated.

3. Illustrative examples

Various mixed models were applied to compute uni-axial buckling loads of simply supported sandwich plates. Two types of buckling modes viz. general buckling and the wrinkling modes were assessed for every sandwich plate. Generally, the overall buckling load for thin as well as moderately thick square panels corresponds to the wave numbers m and n equal to unity. The possibility of wrinkling has been assessed by increasing the value of wave number m in steps of one. The sandwich plate would fail in the wrinkling mode if the critical load with higher wave number is less than the overall buckling load. The wave number n has been considered to be unity for both the types of buckling of all the panels. Present results have been validated by comparing them with the 3-D elasticity, experimental and other analytical solutions available in the literature. The errors involved due to typical simplifying assumptions have been highlighted.

Different material property sets considered in the illustrative examples have been tabulated under Table 1. Uni-axial buckling loads have been expressed in terms of non-dimensional parameters λ_u and λ'_u for a consistent comparison such that

$$\lambda_u = \frac{P_{xcr}L_y^2}{E_{f2}H^3} \tag{15a}$$

$$\lambda'_u = \frac{P_{xcr}L_y^2}{\pi^2 D} \tag{15b}$$

Table 1
Various material property sets used in the illustrative examples

Material set	Properties			
1	*Face sheets—orthotropic* $E_1/E_2 = 19$, $E_3 = E_2$, $G_{12}/E_2 = G_{13}/E_2 = 0.52$, $G_{23}/E_2 = 0.338$, $v_{12} = v_{13} = 0.32$, $v_{23} = 0.49$ *Core—orthotropic* $E_1/E_{2f} = 3.2 \times 10^{-5}$, $E_2/E_{2f} = 2.9 \times 10^{-5}$, $E_3/E_{2f} = 0.4$, $G_{12}/E_{2f} = 2.4 \times 10^{-3}$, $G_{13}/E_{2f} = 7.9 \times 10^{-2}$, $G_{23}/E_2 = 6.6 \times 10^{-2}$, $v_{12} = 0.99$, $v_{13} = v_{23} = 3 \times 10^{-5}$ (*Source*: Noor et al., 1994)			
2	Isotropic aluminium face plate—$E = 70,000$ MPa, $v = 0.3$, $H_{ply} = 0.65$ mm CFRP face plate—$E_1 = 142$ GPa, $E_2 = E_3 = 9.8$ GPa, $v_{12} = v_{13} = v_{23} = 0.34$, $G_{12} = G_{13} = G_{23} = 4.3$ GPa, $H_{ply} = 0.125$ mm Core I—$E_1 = E_2 = G_{12} = 1 \times 10^{-5}$ MPa, $v_{12} = v_{13} = v_{23} = 1 \times 10^{-5}$ $E_3 = 298$ MPa, $G_{13} = 60$ MPa, $G_{23} = 35.2$ MPa, $H_c = 5$ mm Core II—$E_1 = E_2 = G_{12} = 1 \times 10^{-5}$ MPa, $v_{12} = v_{13} = v_{23} = 1 \times 10^{-5}$, $E_3 = 109$ MPa, $G_{13} = 26.6$ MPa, $G_{23} = 15.5$ MPa, $H_c = 25$ mm Adhesive layer—$E = 3050$ MPa, $v = 0.3$ (*Source*: Hadi and Matthews, 2000)			
3	*Face sheets—orthotropic* $E_1 = 131$ GPa, $E_3 = E_2 = 10.34$ GPa, $v_{23} = 0.49$, $v_{12} = v_{13} = 0.22$, $G_{12} = 6.895$ GPa, $G_{13} = 6.205$ GPa, $G_{23} = 6.895$ GPa, *Core—isotropic* $E_1 = E_2 = E_3 = 6.89 \times 10^{-3}$, $G_{12} = G_{13} = G_{23} = 3.45 \times 10^{-3}$, $v_{12} = v_{13} = v_{23} = 1 \times 10^{-5}$ (*Source*: Kant and Swaminathan, 2000)			
4	*Face sheets—isotropic* $E/G_c = 100$ or 1000, $v = 0.3$ *Core—isotropic* $E_c/G_c = 2.6$, $v = 0.3$ (*Source*: Frostig, 1998)			
5	No.	Thickness in mm	E_f in MPa	v
	Properties of isotropic stiff layers			
	1	1.270	0.2068×10^6 (30×10^6 psi)	0.3
	2	1.905	0.0689×10^6 (10×10^6 psi)	0.3
	3	2.540	0.0689×10^6 (10×10^6 psi)	0.3
	4	1.524	0.2068×10^6 (30×10^6 psi)	0.3
	Properties of isotropic cores			
			G_c in MPa	
	1	5.08	68.9442 (1.0×10^4 psi)	0.00001
	2	6.35	55.1553 (0.8×10^4 psi)	0.00001
	3	5.08	82.7330 (1.2×10^4 psi)	0.00001
	(*Source*: Lundgren and Salama, 1971)			

Here, P_{xcr} is the critical load in the x-direction and D is the flexural rigidity of the plate given by

$$D = \sum_{i=1}^{NSL} \frac{E_{fxi} d_i^2 t_{fi}}{(1 - v_{fxyi}^2)} \tag{16}$$

where NSL represents number of stiff layers in a sandwich, E_{fxi} is the modulus of elasticity of ith stiff layer in x-direction, d_i and t_{fi} are its distance from the neutral surface and the thickness, respectively, and v_{fxyi} is the Poisson's ratio in plane xy.

3.1. Example 1: Sandwich plate with laminated cross-ply face sheets and an orthotropic core

A square symmetric sandwich plate of material 1 mentioned under Table 1 has been analyzed for general as well as wrinkling type of buckling. The plate $[(0°/90°)_5/\text{core}/(90°/0°)_5]$ consists of equal thickness cross-ply laminated face sheets with 10 layers and a honeycomb, titanium core. Discretization of each layer of the face into three sub-layers and the core into 10 sub-layers was found to yield converging solutions for HYF1 models. However, such divisions did not improve results when HYF2 models were used.

Noor et al. (1994) have presented 3-D elasticity solutions for the global buckling mode ($m = n = 1$) for the uniform uni-axial edge compressive stress σ_x^p applied to the panel. However, if the pre-buckling deformation is assumed to consist of a uniform strain state and Poisson's ratios of all the layers are considered to be identical, the relative edge stresses in the individual layers are proportional to the respective elastic moduli (Noor, 1975). The in-plane flexural rigidity of cores is comparatively very small and hence the condition of uniform pre-buckling strain is more realistic for sandwiches. Therefore, the sandwich panels are analyzed for the following two loading conditions in the present example.

Case (I) Uniform state of stress in which all the layers are subjected to equal edge stresses; and
Case (II) Uniform state of strain in which the individual layers are subjected to stresses in proportion to their elastic moduli.

The 3-D elasticity results have been presented graphically by Noor et al. (1994). The digitized data from the graph and the general buckling and the wrinkling stress parameters obtained by the present mixed formulations have been tabulated under Table 2. The buckling wave number m has been presented in parenthesis along with each buckling load parameter. The first buckling load (with $m = 1$) has been presented for each case for a consistent comparison with the available 3-D elasticity results. Other buckling load, if any, obtained with higher wave number m, represents the lowest buckling load for that particular case.

The general buckling load parameters obtained by HYF13 model for Case I are in excellent agreement with the 3-D elasticity results. On the other hand, results from case II reveal that the thick sandwich plates considered in the present example buckle at lower stresses in the wrinkling mode particularly, when the ratio of H_f/H is small. Results obtained by the HYF23 model based on ESL theory are higher and non-conservative as compared to those obtained by HYF13 model, which are based on ILT. The difference in the results from these models is large for the wrinkling condition. Further, the difference increases with increase in the thickness of face sheets.

Thus, it can be concluded from the present example that the ILT based, HYF13 model predicts results that are in excellent agreement with the 3-D elasticity results. Further, the model is also capable of predicting the wrinkling behavior. On the contrary, results obtained by the HYF23 model reveals that the ESL theories fail to accurately evaluate overall buckling as well as wrinkling loads in sandwiches. Finally, as the in-plane flexural rigidity of cores is generally very small, the condition of uniform pre-buckling strain seems more realistic for the stability analysis of sandwiches. Therefore, this condition of loading has been assumed in all the examples presented below.

Table 2
Buckling load parameter λ_u for square, symmetric sandwich plate in Example 1

H_f/H	L_x/H	3-D Elast.[a]	Case I		Case II	
			HYF13	HYF23	HYF13	HYF23
0.025	20	2.5543 (1)	2.5563 (1)	2.6538 (1)	2.5390 (1)	2.6386 (1)
	10	2.2376 (1)	2.2370 (1)	2.3362 (1)	2.1904 (1)	2.2942 (1)
		NA	–	–	1.2766 (57)	1.4395 (54)
	20/3	1.8438 (1)	1.8577 (1)	1.9547 (1)	1.7952 (1)	1.8980 (1)
		NA	–	–	0.5680 (38)	0.6407 (36)
	5	1.5027 (1)	1.5063 (1)	1.5971 (1)	1.4427 (1)	1.5393 (1)
		NA	–	–	0.3200 (28)	0.3611 (27)
0.05	20	4.6590 (1)	4.6645 (1)	4.8067 (1)	4.6386 (1)	4.7857 (1)
	10	3.7375 (1)	3.7307 (1)	3.8919 (1)	3.6759 (1)	3.8475 (1)
		NA	–	–	2.8002 (43)	3.4713 (37)
	20/3	2.7911 (1)	2.8079 (1)	2.9668 (1)	2.7506 (1)	2.9222 (1)
		NA	–	–	1.2456 (29)	1.5440 (25)
	5	2.0816 (1)	2.0915 (1)	2.2327 (1)	2.0426 (1)	2.1977 (1)
		NA	1.9028 (2)	–	0.7016 (22)	0.8697 (19)
0.075	20	6.4224 (1)	6.4212 (1)	6.5872 (1)	6.3914 (1)	6.5644 (1)
	10	4.7637 (1)	4.7955 (1)	4.9962 (1)	4.7433 (1)	4.9580 (1)
		NA	–	–	4.6321 (39)	–
	20/3	3.3729 (1)	3.3859 (1)	3.5788 (1)	3.3385 (1)	3.5466 (1)
		NA	3.2527 (2)	3.4788 (2)	2.0595 (26)	2.6357 (21)
	5	2.3973 (1)	2.4052 (1)	2.5655 (1)	2.3672 (1)	2.5461 (1)
		NA	2.0508 (2)	2.2028 (2)	1.1597 (19)	1.4839 (15)
0.100	20	7.8969 (1)	7.8939 (1)	8.0771 (1)	7.8631 (1)	8.0544 (1)
	10	5.6081 (1)	5.5931 (1)	5.8259 (1)	5.5463 (1)	5.7946 (1)
	20/3	3.7883 (1)	3.7813 (1)	3.9951 (1)	3.7424 (1)	3.9752 (1)
		NA	3.4711 (2)	3.7026 (2)	2.9284 (25)	–
	5	2.6051 (1)	2.6101 (1)	2.7824 (1)	2.5789 (1)	2.7719 (1)
		NA	2.1553 (2)	2.2959 (2)	1.6483 (19)	2.1324 (14)

'NA' indicates the results are not available.
'–' indicates λ_u is not minimum in the higher modes.
[a] Digitized data from the graph given by Noor et al. (1994).

3.2. Example 2: Comparison with experimental results

Pearce and Webber (1973) have presented experimental overall buckling and wrinkling loads for sandwich panels, simply supported on all the four edges. The panels were of size $L_x = L_y = 228$ mm and composed of various layers of material 2 as follows:

Overall buckling specimens
Panel (1) Aluminium face plates and core—I
Panel (2) (0°/90°/0°) carbon fiber reinforced polymer (CFRP) face plates and core—I
Wrinkling specimens
Panel (3) Aluminium face plates and core—II
Panel (4) 0° CFRP face plates and core—II
Panel (5) (0°/90°) CFRP face plates and core—II

Thickness of each ply of the face sheets corresponds to those mentioned in material set 2 except for panel 4 where the thickness of face sheet is 0.25 mm. The experimental loads and the loads estimated by various

Table 3
Overall buckling loads in N/mm for the panels considered in Example 2

Panel no.	Expt.[a]	HYF13	HYF23	Anal. I[b]	Anal. II[c]
1	234	298.09 (1)	514.46	243	298
		[353.42] (1)	[593.07]	NA	[302]
		299.42 (2)	658.81	NA	NA
		[353.44] (2)	[733.35]	NA	NA
2	185	136.81	147.95	152	136.9
		[167.69]	[179.03]	NA	[156]

NA indicates results are not available.
[] results with incorporation of adhesive layers.
[a] Experimental results, Pearce and Webber (1973).
[b] Analytical results, Pearce and Webber (1973).
[c] Analytical results, Hadi and Matthews (2000).

Table 4
Wrinkling loads in N/mm for the panels considered in Example 2

Panel no.	Expt.[a]	HYF13	HYF23	Anal. I[b]	Anal. II[c]
3	361	494.04 (19)	566.36 (19)	490	497
		[515.43] (19)	[585.96] (19)	NA	NA
4	191	157.60 (35)	184.29 (35)	160	161.3
		[178.98] (32)	[207.27] (33)	NA	[183.8]
5	137	76.23 (49)	91.03 (51)	77	77.43
		[127.08] (38)	[148.74] (39)	[117]	[130.4]

NA indicates results are not available.
[] results with incorporation of adhesive layers.
[a] Experimental results, Pearce and Webber (1973).
[b] Analytical results, Pearce and Webber (1973).
[c] Analytical results, Hadi and Matthews (2000).

mixed models are presented in Table 3 for overall buckling and in Table 4 for wrinkling conditions. The analytical results obtained by Hadi and Matthews (2000) and Pearce and Webber (1973) are also presented for comparison.

Results obtained by the above two approaches are in good agreement with those obtained by HYF13 model. However, these analytical approaches are based on the typical simplifying assumptions that neglect the transverse energies of the faces and the in-plane energies of the core. Therefore, such approaches are applicable to sandwiches having thin faces and honeycomb type of core having negligible in-plane rigidities. Incorporation of adhesive layers in the analysis improves accuracy of the results.

The experimental overall buckling load for panel 1 with aluminium faces is less compared to the present results. The experimental error can be attributed to the development of transverse stresses in the direction perpendicular to the direction of application of the external stresses due to the Poisson's effect. Such an effect would be less prominent in orthotropic faces where the stiffness in the transverse direction is comparatively less. Panel 1 was observed to buckle in two half waves during overall buckling (Pearce and Webber, 1973) which has been confirmed by the HYF13 model as the overall buckling loads for the first two modes are more or less equal. The experimental overall buckling load for the second panel is greater than the present as well as the other analytical results. It may be due to the effect of end restraint provided by the end blocks. Such an effect is less predominant in the first panel that buckled in two half waves. A similar trend in the results can also be observed from Table 4 for the wrinkled specimens.

3.3. Example 3: Sandwich plate with laminated cross-ply face sheets and an isotropic core

Uni-axial buckling load parameter λ_u of a square [0°/90°/core/90°/0°] sandwich plate of material 3 having $H_c/H_f = 10$ has been presented in Table 5. Here, H_c and H_f are thicknesses of the core and one complete face sheet, respectively. Results obtained by Kant and Swaminathan (2000) by using displacement based higher-order ESL theory (HSDT) have also been presented for comparison. They have considered only the general buckling mode with mode numbers (1, 1). These results are in good agreement with the present ESL model HYF23. However, it can be observed from Table 5 that the minimum general buckling loads would be obtained at higher modes. The general buckling loads obtained by the ILT (HYF13 model) are less than those obtained by the ESL theory (HYF23 model) because the ratio of E_{f1}/G_c is as high as 37,971 for the sandwich plate under consideration. Such high ratio indicates a soft core. Difference in the general buckling parameters obtained by the two approaches was found to reduce when L_x/H was increased. Thus, it may be concluded from the present example that even though higher-order formulation is employed, the ESL theories might fail to accurately predict the buckling loads for soft core sandwiches due to a vast difference in the material properties of the faces and the core.

Table 5
Buckling load parameter λ_u for square, symmetric sandwich plate in Example 3

L_x/H	HYF13	HYF23	HSDT[a]
2	0.0109	0.0325	0.0315
	–	0.0224 (2)	NA
4	0.0190	0.1014	0.0972
	–	0.0786 (2)	NA
10	0.0749	0.5409	0.5181
	0.0585 (2)	0.3761 (3)	NA
20	0.2659	1.6775	1.6220
	0.1862 (3)	1.3392 (3)	NA
30	0.5576	2.7719	2.6932
	0.3801 (3)	2.6517 (2)	NA
40	0.9181	3.5961	3.5256
	0.6457 (3)	–	NA
50	1.3150	4.1712	4.1139
	0.9775 (3)	–	NA
60	1.7209	4.5685	4.5323
	1.3694 (3)	–	NA
70	2.1156	4.8471	4.8091
	1.8145 (3)	–	NA
80	2.4862	5.0470	5.0164
	2.2569 (2)	–	NA
90	2.8260	5.1938	5.1657
	2.7109 (2)	–	NA
100	3.1324	5.3042	5.2794
	3.1687 (2)	–	NA

– indicates buckling load parameter in the higher mode is not minimum.
NA indicates the results are not available.
[a] Kant and Swaminathan (2000).

3.4. Example 4: Sandwich plate with isotropic face sheets and an isotropic core

Uni-axial buckling load parameter λ'_u of a sandwich plate with $L_y/H = 14.96$ and $H/H_f = 40.1$ have been presented in Table 6. The plate consists of isotropic faces of equal thickness and an isotropic core. The results have been obtained for $E_f/G_c = 100$ as well for $E_f/G_c = 1000$ indicating a strong and a weak core, respectively. It can be observed from the results of both the mixed models that the response of the sandwich plate with $E_f/G_c = 100$ corresponds to an overall buckling mode. On the other hand, the sandwich plate having $E_f/G_c = 1000$ has been observed to buckle in a wrinkling mode with high mode numbers. The overall buckling loads obtained by Allen (1969) are in good agreement with the results obtained by HYF13 model, particularly, for $E_f/G_c = 1000$. However, the overall buckling loads obtained by Allen (1969) for smaller values of E_f/G_c are relatively less due to the typical simplifying assumptions of ignoring the out-of-plane energies of the faces and the in-plane energies of the core. Further, the wrinkling behavior cannot be predicted by the zigzag three-layer model presented by Allen (1969). The results obtained by Frostig (1998) by using a higher-order theory are too low as the formulation has been based on simplifying assumptions except that energy of the core associated with the transverse normal stress (σ_z) has been incorporated. Moreover, the results indicate a wrinkling behavior in both the panels. Therefore, the wrinkling loads obtained by Frostig (1998) for the panel having $E_f/G_c = 100$ can be attributed to the simplifying assumptions and may not represent the true behavior of the sandwich plate. Thus, it may be concluded that the simplifying assumptions may either lead to too conservative results or prediction of a wrong buckling mode, especially, for isotropic cores having small E_f/G_c.

The normalized displacements and stresses obtained by the HYF13 model have been plotted in Fig. 2(a)–(e) for a square sandwich plate with $L_x/H = L_y/H = 14.96$, $E_f/G_c = 100$ subjected to overall buckling ($m = 1$). These parameters are plotted in Fig. 3(a)–(e) for a similar plate with $E_f/G_c = 1000$ subjected to wrinkling at mode number $m = 39$. A marked difference in the transverse stress variation can be observed from Figs. 2(e) and 3(e) for the two types of buckling modes. The variation of the in-plane displacements for the wrinkling mode has been indicated in Fig. 3(a) and it does not match with the variation assumed in

Table 6
Buckling load parameter λ'_u for the sandwich plate considered in Example 4

L_x/L_y	$E_f/G_c = 100$				$E_f/G_c = 1000$			
	HYF13	HYF23	Allen[a]	Frostig[b]	HYF13	HYF23	Allen[a]	Frostig[b]
0.5	5.3295 (1)	5.5109	4.8574	NA	1.6164 (1)	1.8534	1.6161	NA
	–	–	–	1.9413	1.0648 (19)	–	NA	0.6481
1.0	4.0432 (1)	4.1256	3.5888	NA	1.6164 (2)	1.8534	1.6161	NA
	–	–	–	1.9413	1.0646 (39)	–	NA	0.6481
1.5	4.1844 (2)	4.2860	3.7443	NA	1.6164 (3)	1.8534	1.6161	NA
	–	–	–	1.9413	1.0646 (58)	–	NA	0.6481
2.0	4.0432 (2)	4.1256	3.5888	NA	1.6164 (4)	1.8534	1.6161	NA
	–	–	–	1.9413	1.0646 (77)	–	NA	0.6481
2.5	4.0674 (3)	4.1595	3.6273	NA	1.6164 (5)	1.8534	1.6161	NA
	–	–	–	1.9413	1.0646 (97)	–	NA	0.6481

– indicates buckling load parameter in the higher mode is not minimum.
NA indicates the results are not available.
[a] Allen (1969).
[b] Frostig (1998).

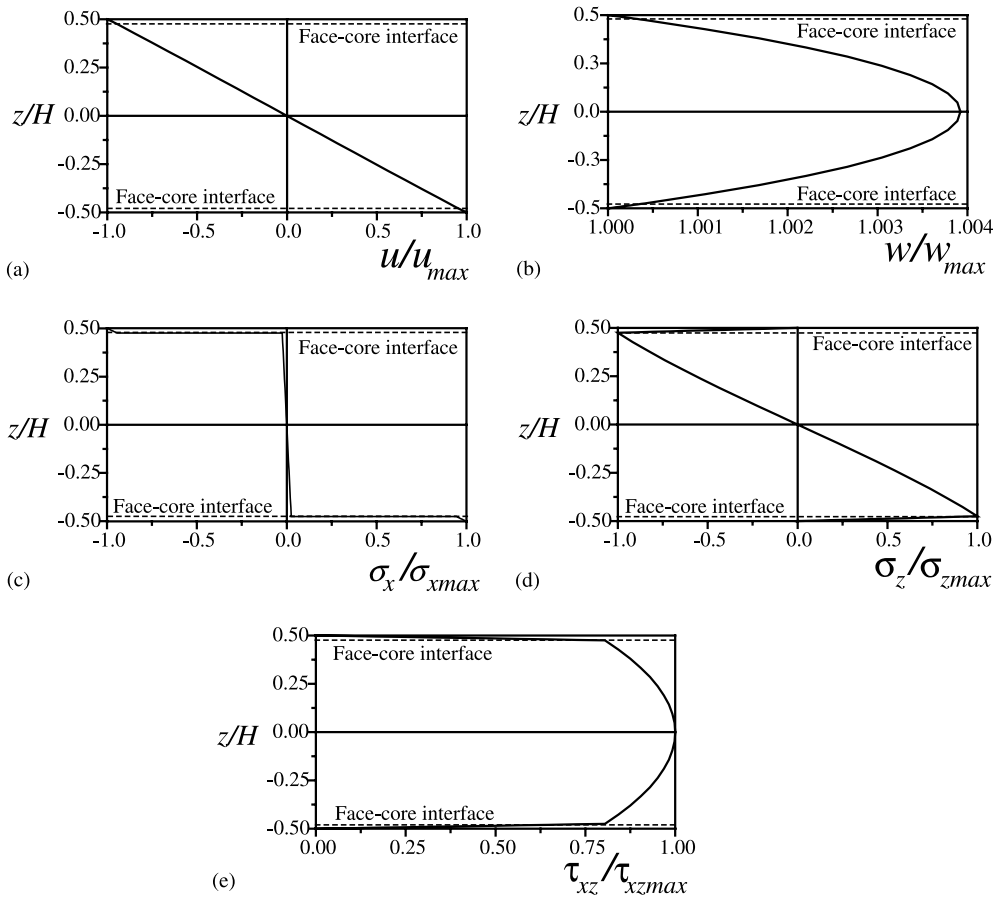

Fig. 2. Variation of the normalized: (a) in-plane displacement ($u/u_{\max}$); (b) transverse displacement (w/w_{top}); (c) in-plane stress ($\sigma_x/\sigma_{x\max}$); (d) transverse normal stress ($\sigma_z/\sigma_{z\max}$); and (e) transverse shear stress ($\tau_{xz}/\tau_{xz\max}$) for the sandwich plate ($E_f/G_c = 100$) in Example 4 subjected to overall buckling.

the ESL theories. Thus, the ESL theories cannot accurately model the wrinkling behavior of sandwiches as revealed by the results of the HYF23 model.

3.5. Example 5: Unsymmetric, multi-layer, multi-core sandwich plate

Uni-axial critical buckling loads ($P_{x\text{cr}}$) for a seven-layer sandwich plate (material 5) have been presented in Table 7. The plate has been analyzed for $L_y = 2.54$ m (100 in.) for different values of L_x. Results obtained by the following approaches have also been presented for comparison.

(i) FSM by Chan and Foo (1977); and
(ii) Series solutions by Wong and Salama (1967).

Results obtained by the FSM (Chan and Foo, 1977) are in good agreement with the results of HYF13 model. However, the finite strip formulation is based on the typical simplifying assumptions. Wong and Salama (1967) obtained the buckling loads of the multi-layer multi-core sandwich plate by assuming a

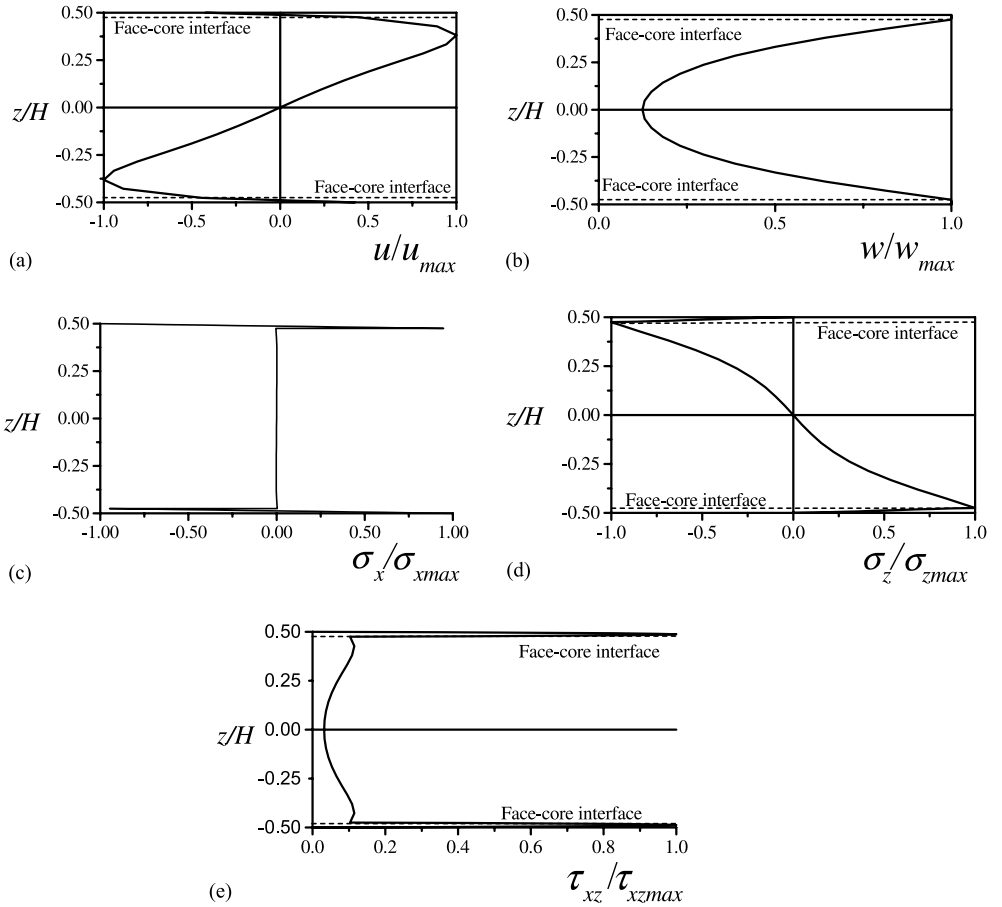

Fig. 3. Variation of the normalized: (a) in-plane displacement ($u/u_{\max}$); (b) transverse displacement (w/w_{top}); (c) in-plane stress ($\sigma_x/\sigma_{x\max}$); (d) transverse normal stress ($\sigma_z/\sigma_{z\max}$); and (e) transverse shear stress ($\tau_{xz}/\tau_{xz\max}$) for the sandwich plate ($E_f/G_c = 1000$) in Example 4 subjected to wrinkling.

Table 7
Buckling load (P_{xcr}) in kN for an unsymmetric multi-layer sandwich plate considered in Example 5

L_x/L_y	HYF13	HYF23	FSM[a]	Series solution[b]
0.4	17.5662 (1)	27.6759	18.7439	15.0677
0.7	12.0237 (1)	14.9620	12.4651	11.0440
1.0	11.3829 (1)	13.2204	11.7007	10.7030
1.2	12.0255 (1)	13.6682	12.3308	11.3901
1.6	14.7186 (1)	16.3706	15.0689	14.0522
	11.5104 (2)	13.8833	NA	NA
2.0	18.7672 (1)	20.6698	19.2168	17.9935
	11.3829 (2)	13.2204	NA	NA

NA indicates the results are not available.
[a] Chan and Foo (1977).
[b] Wong and Salama (1967).

common shear angle for all the cores in addition to the typical simplifying assumptions. Moreover, both the approaches seem to presume that the minimum buckling load occurs at the mode number $m = 1$. On the contrary, longer plates tend to buckle in higher modes dividing the plate into approximately square panels. Finally, as expected, the results obtained by the present ESL model (HYF23) are comparatively high.

4. Conclusions

A unified mixed, higher-order analytical formulation has been developed by using the minimum potential energy principle for stability analysis of sandwich plates. Continuity of displacements as well as the transverse stresses through thickness has been explicitly satisfied in the formulation. The proposed ILT (HYF13 model) appears to accurately evaluate the overall buckling as well as wrinkling loads of sandwiches. On the contrary, results obtained by various ESL theories indicate that such theories cannot accurately predict the wrinkling loads of sandwiches. Moreover, the over-all buckling loads obtained by such theories are higher and non-conservative particularly, for the soft-core sandwiches due to a vast difference in the material properties of the faces and the core. Therefore, it may be concluded that the ESL theories that are adequate for the analysis of laminated composite plates, fail to accurately evaluate the overall buckling as well as wrinkling response of sandwiches. Further, the usual assumptions of stiff layers and anti-plane core may lead either to too conservative results or to prediction of a wrong buckling mode, especially, for isotropic cores having small values of E_f/G_c ratios indicating a relatively strong core. Finally, a marked difference in the variations of in-plane displacements and the transverse stresses has been observed in the two modes of buckling of sandwiches. The wrinkling phenomenon is associated with compressibility of cores. Therefore, an assumption of constant transverse displacement cannot lead to prediction of wrinkling behavior in sandwiches.

Acknowledgements

The work presented in this paper has been sponsored by project sanctioned by the Ministry of Human Resource Development, INDIA (Grant No. 02MH018). Support was also received from ISIS CANADA (Intelligent Sensing for Innovative Structures, A Canadian Research Network of Centres of Excellence). Constructive comments of the reviewers are gratefully acknowledged.

References

Aiello, M.A., Ombres, L., 1997. Local buckling loads of sandwich panels made with laminated faces. Composite Structures 38 (1–4), 191–201.

Allen, H.G., 1969. Analysis and Design of Structural Sandwich Panels. Pergamon Press, London.

Benson, A.S., Mayers, J., 1967. General instability and face wrinkling of sandwich plates—unified theory and applications. AIAA Journal 5 (4), 729–739.

Chan, S.C., Foo, O., 1977. Buckling of multi-layer sandwich plates by the finite strip method. International Journal of Mechanical Sciences 19, 447–456.

Dafedar, J.B., Desai, Y.M., 2002. Thermo-mechanical buckling of laminated composite plates using mixed, higher-order analytical formulation. ASME Journal of Applied Mechanics 69 (6), 790–799.

Frostig, Y., 1998. Buckling of sandwich panels with a flexible core-high-order theory. International Journal of Solids and Structures 35 (3–4), 183–204.

Hadi, B.K., Matthews, F.L., 1998. Predicting the buckling load of anisotropic sandwich panels: an approach including shear deformation of the faces. Composite Structures 42, 245–255.

Hadi, B.K., Matthews, F.L., 2000. Development of Benson–Mayer theory on the wrinkling of anisotropic sandwich panels. Composite Structures 49, 425–434.

Hunt, G.W., Da Silva, L.S., 1990. Interactive buckling in sandwich structures with core orthotropy. International Journal of Mechanical Structures and Mechanics 18 (3), 353–372.

Hunt, G.W., Da Silva, L.S., Manzocchi, G.M.E., 1988. Interactive buckling in sandwich structures. Proceedings of the Royal Society, London A 417, 155–177.

Kant, T., Swaminathan, K., 2000. Analytical solutions using a higher order refined theory for the stability analysis of laminated composite and sandwich plates. Structural Engineering and Mechanics 10 (4), 337–357.

Kim, C.G., Hong, C.S., 1988. Buckling of unbalanced anisotropic sandwich plates with finite bonding stiffness. AIAA Journal 26 (8), 982–988.

Ko, W.L., Jackson, R.H., 1993. Compressive and shear buckling analysis of metal matrix composite sandwich panels under different thermal environments. Composite Structures 25, 227–239.

Lundgren, H.R., Salama, A.E., 1971. Buckling of multi-layer plates by finite elements. Journal of Engineering Mechanics, ASCE 97 (2), 477–494.

Noor, A.K., 1975. Stability of multilayered composite plates. Fiber Science Technology 8 (2), 81–89.

Noor, A.K., Burton, W.S., 1996. Computational models for sandwich panels and shells. Applied Mechanics Reviews 49 (3), 155–199.

Noor, A.K., Peters, J.M., Burton, W.S., 1994. Three-dimensional solutions for initially stressed structural sandwiches. Journal of Engineering Mechanics, ASCE 120 (2), 284–303.

Pearce, T.R.A., Webber, J.P.H., 1971. Buckling of sandwich panels with laminated face plates. Aeronautical Quarterly 23 (2), 143–161.

Pearce, T.R.A., Webber, J.P.H., 1973. Experimental buckling loads for sandwich panels. Aeronautical Quarterly (November), 295–312.

Rao, K.M., 1985. Buckling analysis of anisotropic sandwich plates faced with fiber-reinforced plastics. AIAA Journal 23 (8), 1247–1253.

Wong, J.P., Salama, A.E., 1967. Stability of multi-layer sandwich plates. Journal of Engineering Mechanics, ASCE 93 (3), 19–31.